

Małgorzata Krówczyńska\*, Ewa Wilk\*, Piotr Pabjanek\*, Marlena Kycko\*

## Hyperspectral Discrimination of Asbestos-Cement Roofing

### 1. Introduction

Asbestos is characterised by a unique set of physical and chemical properties, which has led to its many applications [28], such as roofing coatings: flat and corrugated sheets, floors, water supply pipes, textiles, rope, cord and yarn, paper, friction and composition materials, household products, plastic fillers, clutches, brake linings, gaskets and pads for automobiles [30]. Asbestos-cement roofing, and building construction materials represent the majority of currently used asbestos-containing products in the world [5]. Exposure to asbestos and asbestos dust causes a wide range of diseases, such as mesothelioma, asbestosis, and lung cancer [16]. Since asbestos-containing products were proved to be harmful to human health, their usage and production was banned in 55 countries, including from January 1, 2005 all EU countries [6, 15, 20]. In Poland, in particular, asbestos production and trade was forbidden in 1997 [1, 15]. Nevertheless, there are still about 14.5 mln tons of asbestos containing products used across the country [25]; based on estimations performed on asbestos mineral imports data into Poland.

Asbestos-cement roofing discrimination forms the part of the classification issue of built-up areas, including a detailed investigation of different types of roofing. Built-up areas are of interest of many researchers, both in relation to urban and rural areas. Ben-Dor et al. [3] acquired spectral library from 400 nm to 1100 nm of urban surfaces, and have discussed the significance of spectral regions in mapping urban areas, concluding that urban objects bear spectral fingerprints in the spectral region enabling reasonable spectral recognition. Marino et al. [21] have tested the MIVIS (Multispectral Infrared and Visible Imaging Spectrometer) airborne hyperspectral scanner to map asbestos concrete sheeting. Segl et al. [26] have proposed the incorporation of shape characteristics of urban surface materials in order to increase the reliability of buildings identification and to improve the results of spatial

---

\* University of Warsaw, Faculty of Geography and Regional Studies, Department of Geoinformatics, Cartography and Remote Sensing, Warsaw, Poland

distribution of urban surface cover types. Herold et al. [14] have developed and analysed the spectral library from 350 nm to 2400 nm of roofs, roads, parking lots, vegetation and bare soil; and adopted the division of buildings/roofs typical for the vicinity of Santa Barbara, CA, US, taking into consideration the composite material (composite shingle, plastic, glass, gravel, metal, asphalt, tile, tar and wood shingle) and colour (shingle: black, blue, brown, green, grey, orange, red, tan, white; metal: brown, light grey, green; tile: red, grey; tar: black, brown; wood shingle: dark), however the main aim of the survey was to determine the spectral features of urban materials. The undertaken survey has revealed some limitations in abstracting urban materials; the authors suggested further detailed investigation into using hyperspectral data in urban area mapping. Composite material and colour of roofing were examined by Heiden et al. [11]. The vast number of spectral features was established for bright materials. It was found difficult to separate dark composite materials, and emphasized that urban material description should be executed by more than one type of the leading feature. So far undertaken surveys on urban areas incorporate roofing materials as an essential issue in urban area mapping, however, in particular they do not provide guidelines with the leading feature to distinguish ACR. Bassani et al. [2] have demonstrated that remote sensing data are useful for the purposes of identifying corrugated ACR sheets and the evaluation of asbestos fibre air dispersion as the cause of lung cancer. The authors found that absorption features at 2.32  $\mu\text{m}$  and at 9.44  $\mu\text{m}$  were correlated with asbestos surface with the use of MIVIS spectral data over two industrial test areas in Italy. The determination of the amount of asbestos-containing materials is essential for the landfill development program and the application of adequate policies and monitoring systems. The estimation of the amount asbestos-cement products is raised; in Italy by Fiumi et al. [8, 9], Frassy et al. [10], in Hungary by Szabó et al. [27] and in Poland by Krówczyńska et al. [18].

The aim of this work was to analyse the spectral reflectance curves of roofing used in Poland to determine whether hyperspectral data analysis might have the practical application in the development of an expeditious method of the discrimination of asbestos-cement roofing.

Data were acquired with FieldSpec 3 ASD spectrometer as it gives the opportunity to acquire the continuous measurements of spectral reflectance within the spectral range from 350 nm to 2500 nm, which can be used thereafter for different sensors. Tested features consisted of: construction material, colour, and the outer protective layer of each roof covering. The study presents results on the identification of spectral characteristics of roofing materials that have a significant influence on the shape of spectral reflectance curves [13]. Laboratory measurements of roofing materials spectral curves, wavelengths with maximum spectral reflectance differences between asbestos-cement sheets used in Poland and other roof coverings were executed to determine the possibility of functional distinction of various types of roof coverings on the basis of spectral curves analyses.

## 2. Methods

The undertaken analysis covered the following groups of roofing materials: concrete tile (4 types), ceramic tiles (8 types), sheet metal and roofing sheet (27 types), roofing felt (2 types), and asbestos-cement roofing (two types). There were two types of asbestos-cement roofing used in Poland: flat and corrugated asbestos-cement sheets. Flat asbestos-cement sheets according to the Polish Industry Standard No BN-67/6754-02 contained 10–11% of pure asbestos mineral fibres, and corrugated asbestos-cement sheets – 10–14% [24].

The largest group consisted of metal sheet and roof tiles since they are the most commonly used roofing material in Poland. Roof coverings were divided according to: composite material, colour, and protective coating; abbreviations were assigned to each tested feature: the first letter stands for composite material, the second – for colour, the third for type of protective coating, and the fourth for material structure (if applicable) (Tab. 1).

**Table 1.** Symbols used in the undertaken survey

No.	Composite materials	Colour	Type of protective coating	Structure
1	A – asbestos–cement flat or corrugated sheets	Bd – dark brown	0 – none (natural)	c – extruded
2	B – roofing felt	Bd2 – purple	B – adhesive	–
3	C – clay (ceramic tiles)	Bk – black	C – engobed (enamelled)	–
4	M – metal	Bl – blue	L – lacquered	–
5	T – cement	Br – brown	Pe – poliester	–
6	–	Gd – dark green	Pr – polyurethane–polyamide	–
7	–	Gl – light grey	Px – polyurethane	–
8	–	Gn – green	–	–
9	–	Gs – dark grey	–	–
10	–	Gy – graphite	–	–
11	–	Or – copper	–	–
12	–	Rd – maroon	–	–
13	–	Re – ochre	–	–

The field spectral library of roofing materials between 350 nm and 2500 nm was developed. The halogen ASD ProLamp was the source of radiation imitating sunlight. During measurements, the optical fiber was fixed at 90°, and halogen lamps were mounted at the angle of 45° and 135° relative to the plane of the measurement. Shadow of roofing was not considered since laboratory measurements were done at the distance of 10 cm, where the shadow had no effect on the size of the spectral reflectance.

The performance of laboratory measurements was preceded by spectrometer optimisation; optimisation included among others the selection of the optimal

duration of measurement, dependent on the number of photons reaching the detector, calibration against the pattern of black (Dark Current) to eliminate noises generated by the device, and calibration against the pattern of white, which was the plate covered with Spectralon [19].

Measurements were taken in 10 runs consisted of 10 measurements each. Spectrum averaging provided by FieldSpec® Pro software was performed [7]. The average value was calculated for each series of measurements. Roofing material shape (flat or corrugated) does not affect the size of the rebound since measurements were performed from a height of 10 cm. Therefore size of the rebound was not considered for further examination. Laboratory measurements were executed for 2151 channels for the wavelength range from 350 nm to 2500 nm, and were presented in the form of 43 spectral reflectance curves. Grouping of the spectral reflectance curves using the J.H. Ward's method was done in Statistica 10 software, and based on the Euclidean distance matrix. 6 clusters of similar shape curves were distinguished. J.H. Ward's method supported the connectivity of similar spectral curves providing a quantitative approach [29].

Most methods used for the hyperspectral analysis of urban areas do not directly identify specific features of building construction materials, i.e. composite material, colour and outer protective layer. The analysis of spectral reflectance curves was performed in ENVI 5.0 software with the use of Spectral Angle Mapper and Spectral Feature Fitting algorithms, both implemented in Spectral Analyst (ENVI 5.0 software extension). Spectral analysis allowed for the separation of roofing materials most and least correlated with asbestos-cement roofing.

The spectral angle mapper (SAM) is an algorithm that evaluates similarity between spectral signature by treating them as vectors in an  $n$ -dimensional space where the number of dimensions is equal to the number of bands, and measuring the angle between vectors [4]. Smaller angles represent closer matches to the reference spectrum. On the contrary, the spectral feature fitting (SFF) algorithm measures similarity by the evaluation of the physical shape of spectral signatures and uses continuum removed spectra. For each unknown spectral signature, scale, or measure of absorption feature depth relative to the spectrum is calculated. In addition, the unknown spectral signature is compared at each selected wavelength in a least-squares sense, and the root mean square (RMS) error is determined for each spectrum. Pixels with high scale and low RMS are deemed close matches [22].

In order to assess the possibility of discrimination of ACR from other roof coverings used in Poland, research was undertaken to define the ranges, where the difference of reflectance is greater than 0.1 in comparison to the value of ACR reflectance. It was assumed that the difference in reflectance greater than 0.1 allows for the discrimination of different types of roof coverings by most available sensors. In the case of sensors with a resolution of 8 bits, the difference is 25 shades of grey, and in case of 11-bit image – 204 shades of grey; therefore it was concluded that tonal variation in the classification should allow for the discrimination of different types of roof coverings (Fig. 1).

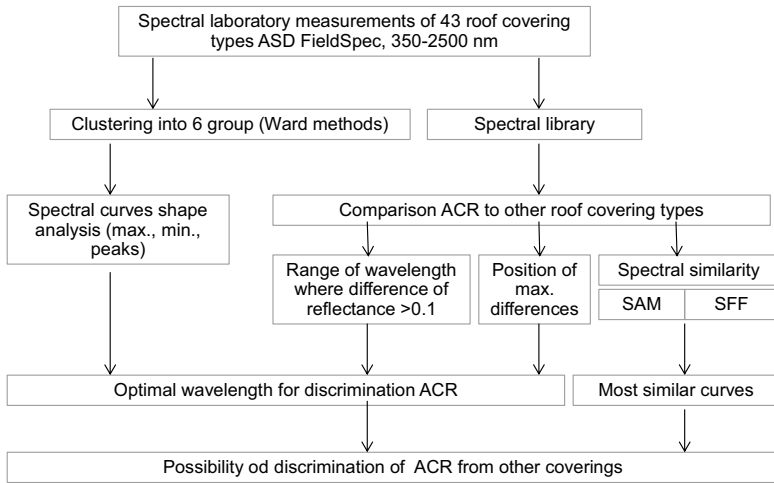


Fig. 1. Flowchart of work

### 3. Results

#### 3.1. Spectral Curves Analysis

In each group different materials, coatings, and colours were taken into consideration under the survey. Graphs presenting the course of spectral curves were developed for each group; asbestos-cement roofing was compared with each group.

Group 1 consists of four black and one dark brown roof covering. The composite material is metal and roofing felt. Spectral reflectance throughout the tested range is very low and aligned, and varies from 0.02 to 0.06 (Fig. 2). In this group the dominant feature is the colour of the roofing.

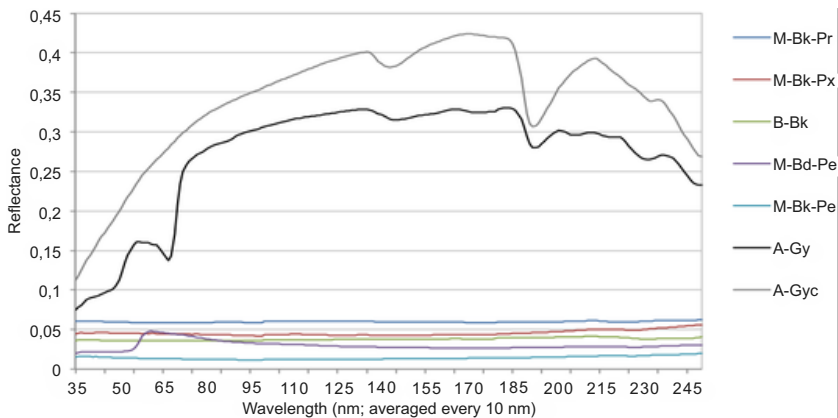


Fig. 2. Group 1 spectral curves (comparison to A-Gy, and A-Gyc spectral curve added)

Group 2 contains grey, dark grey, brown, and dark brown roof coverings made of metal, concrete tile, and roofing felt. Spectral reflectance in the whole tested range is low and aligned from 0.05 to 0.12 (Fig. 3). The colour of roofing is the dominant feature observed in this group.

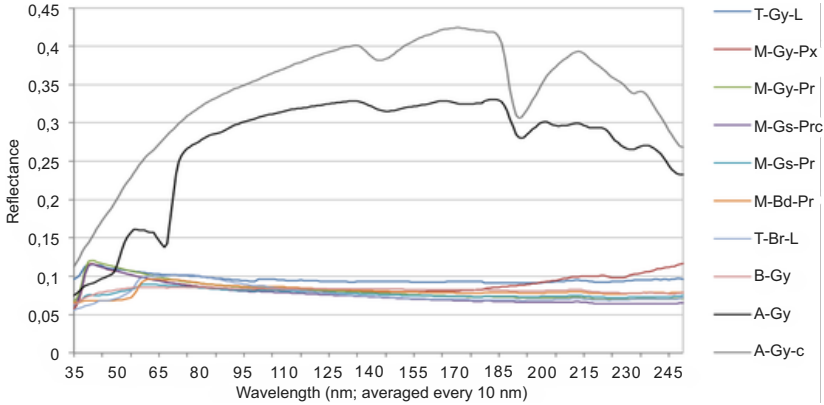


Fig. 3. Group 2 spectral curves (comparison to A-Gy, and A-Gyc spectral curve added)

Group 3 comprises of coloured metal sheets covered with the polyester, polyester-polyurethane, and polyurethane protective coating. It is characterized by a peak in the visible spectrum connected with colour of roof tiles, and increasing reflection along with the wavelength, prevails reflection within the range of 0.05–0.35 (Fig. 4). The peak within the range of 2260–2290 nm is observed (probably typical for polyurethane). Three types of roof coverings in this group are characterized by a greater reflection in the visible, near-infrared spectrum, and a decrease within the range of longer wavelengths (light grey metal sheet coated with polyurethane and polyamide extrusion, dark brown and maroon metal sheet with the coating of polyurethane and polyamide purple, chocolate brown metal sheet coated with polyurethane and polyamide). The leading feature in this group is the composite material and the type of protective coating.

Group 4 consists of asbestos-cement corrugated and flat sheets, and copper and ochre metal sheets with the polyurethane-polyamid protective coating with the similar spectral reflectance within the range of near infrared from 0.2 to 0.45 (Fig. 5). The asbestos-cement and concrete tile roof coverings group has a local minimum within the range 1920–1930 nm. There is no leading feature observed in this group, however, 3 out of 6 roof coverings were made of concrete tile.

Group 5 includes clay, metal (4), and concrete tile roof coverings covered with ochre and copper coating. Spectral reflectance varies from 0.25 to 0.6. There is a peak in the spectral reflectance within the range of 2260 nm to 2280 nm (except of engobed, ochre ceramic tile). The dominant feature in group 5 is the colour of the roofing (Fig. 6).

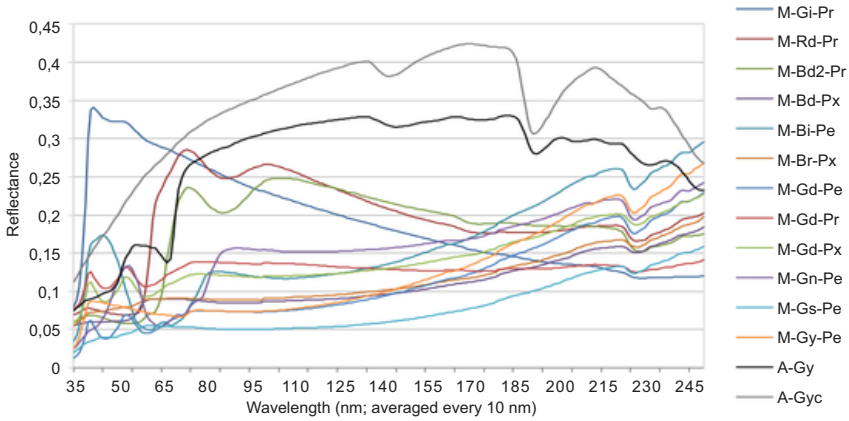


Fig. 4. Group 3 spectral curves (comparison to A-Gy, and A-Gyc spectral curve added)

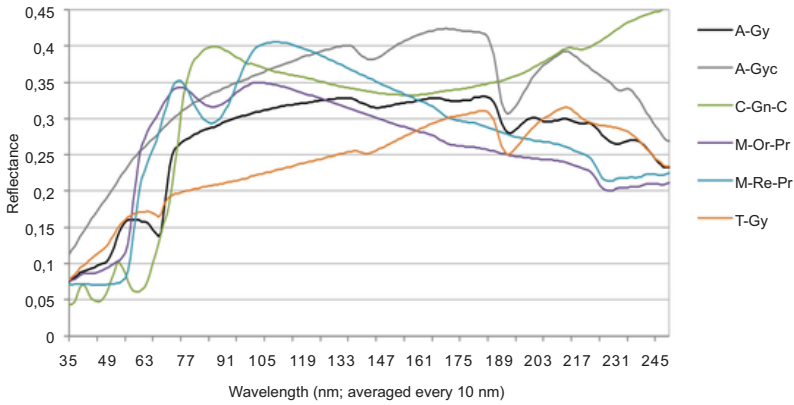


Fig. 5. Group 4 spectral curves (comparison to A-Gy, and A-Gyc spectral curve added)

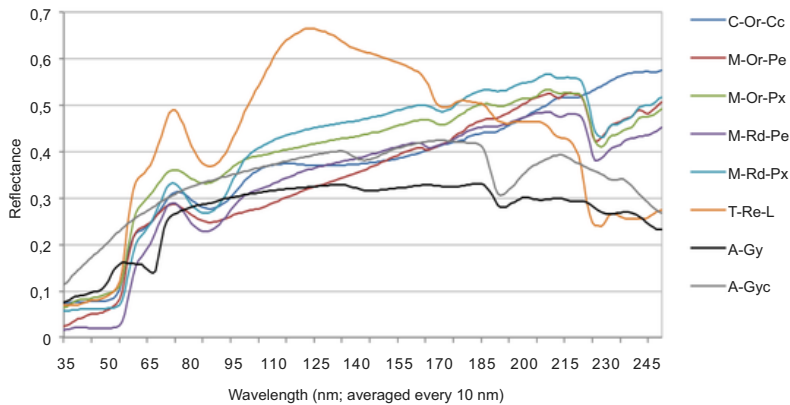


Fig. 6. Group 5 spectral curves (comparison to A-Gy, and A-Gyc spectral curve added)

Group 6 constitutes of ceramic tiles with the highest spectral reflectance in the infrared spectrum up to 0.8 (Fig. 7). Roofing covered with copper and ochre coating have peaks in the red spectrum. Ceramic tiles with dark coatings have lower reflectance rates in the visible spectrum. There is no dominant trait in this group, as it consists of ceramic tiles in different colours (ochre, copper, grey and black), protected with no or various coatings (enamelled, lacquered).

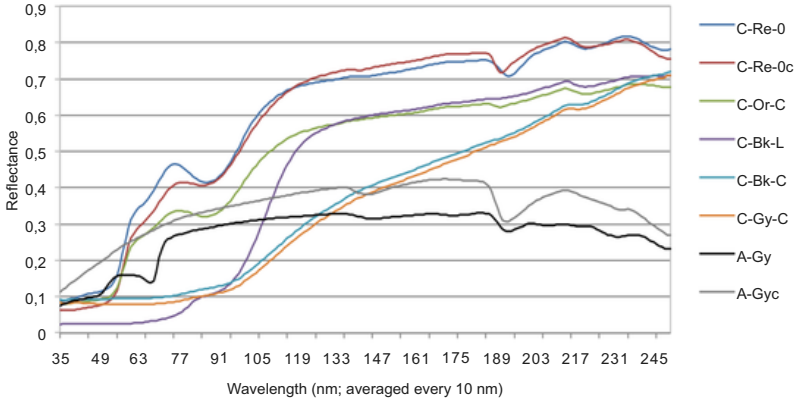


Fig. 7. Group 6 spectral curves (comparison to A-Gy, and A-Gyc spectral curve added)

Great influence on the shape of roof coverings spectral curves has the colour of roofing, and the composite material as well; also the effect on the spectral curve’s shape is noticed for the type of protective coating. Roof tiles coated with polymers have a local minimum within the range of 2250–2300 nm, and for the polyester it amounts to 2267 nm. Asbestos-cement sheets and concrete tile roof coverings, i.e. without any protective coating and colourless, have a local minimum within the range between 1920 nm and 1930 nm.

### 3.2. Spectral Similarity

Application of SAM algorithm has revealed that asbestos-cement flat sheets (A-Gy) are mostly correlated with asbestos-cement corrugated sheets (A-Gyc), purple metal sheets with polyurethane-polyamide protective coating (M-Bd2-Pr) (Tab. 2). The weakest correlation was found for black (C-Bk-L) and grey engobed ceramic tile (C-Gy-C), and light grey metal with polyurethane-polyamide protective coating (M-Gl-Pr). The spectral curve of the asbestos-cement corrugated sheets (A-Gyc) is most similar to the spectral characteristics of the asbestos-cement flat sheets (A-Gy), grey cement tile (T-Gy), and ochre metal coated with polyurethane-polyamide (M-Re-Pr). The lowest correlation was denoted for black (C-Bk-L), and grey engobed ceramic tile (C-Gy-C), and light grey metal sheets with polyurethane-polyamide protective coating (M-Gl-Pr).



**Table 2.** Similarity analysis of roofing material including asbestos-cement flat and corrugated sheets with other roofing materials using Spectral Angle Mapper and Spectral Feature Fitting algorithm

Spectral Angle Mapper				Spectral Feature Fitting			
A-Gy	1.000	A-Gyc	1.000	A-Gyc	1.000	A-Gy	1.000
A-Gyc	0.918	A-Gy	0.918	T-Gy	0.748	C-Gn-C	0.509
M-Bd2-Pr	0.864	T-Gy	0.888	B-Gy	0.565	M-Bd2-Pr	0.461
T-Gy	0.859	M-Or-Px	0.830	M-Gl-Pr	0.522	M-Gd-Pr	0.364
M-Or-Px	0.841	M-Gd-Pr	0.828	T-Br-L	0.522	M-Gn-Pe	0.357
M-Re-Pr	0.827	M-Bd2-Pr	0.820	M-Gs-Pr	0.519	M-Re-Pr	0.325
C-Gn-C	0.808	B-Gy	0.808	M-Bk-Pr	0.518	C-Bk-L	0.323
M-Or-Pr	0.807	B-Bk	0.806	M-Bk-Px	0.515	M-Rd-Pe	0.313
C-Re-U	0.806	M-Re-Pr	0.802	T-Gy-L	0.503	M-Rd-Px	0.307
M-Rd-Px	0.806	M-Or-Pr	0.802	M-Gy-Px	0.502	C-Or-Cc	0.289
M-Gd-Pr	0.794	M-Bd-Pr	0.798	M-Bd-Pe	0.502	C-Re-0c	0.285
C-Re-UC	0.791	C-Re-0	0.794	M-Gd-Pr	0.500	M-Or-Pr	0.278
T-Re-L	0.790	M-Bk-Pr	0.791	M-Br-Px	0.500	C-Re-0	0.274
C-Or-C	0.778	M-Rd-Px	0.787	M-Rd-Pr	0.499	M-Rd-Pr	0.272
M-Rd-Pe	0.774	M-Gs-Pr	0.774	M-Bd-Pr	0.499	T-Gy	0.264
M-Rd-Pr	0.772	C-Re-0c	0.773	M-Gs-Prc	0.499	M-Or-Px	0.261
B-Gy	0.761	T-Re-L	0.772	M-Gy-Pr	0.498	T-Re-L	0.255
B-Bk	0.761	C-Or-C	0.766	M-Bk-Pe	0.496	C-Or-C	0.248
M-Gn-Pe	0.757	M-Bk-Px	0.766	M-Bd-Px	0.492	C-Gy-C	0.236
M-Bd-Pr	0.755	M-Rd-Pr	0.764	M-Gd-Px	0.489	M-Or-Pe	0.234
C-Or-CC	0.748	C-Gn-C	0.761	M-Gs-Pe	0.489	C-Bk-C	0.231
M-Bk-Pr	0.747	M-Rd-Pe	0.753	A-Gy	0.485	M-Bl-Pe	0.225
M-Or-Pe	0.733	M-Gn-Pe	0.750	B-Bk	0.482	M-Gd-Pe	0.220
M-Gs-Pr	0.729	T-Gy-L	0.742	C-Gn-C	0.479	M-Gd-Px	0.211
M-Bk-Px	0.723	C-Or-Cc	0.740	M-Gy-Pe	0.478	M-Bk-Pr	0.209
M-Gd-Px	0.722	M-Gd-Px	0.740	M-Gd-Pe	0.476	M-Bd-Pr	0.189
T-Br-L	0.701	T-Br-L	0.738	C-Or-Cc	0.474	B-Bk	0.180
T-Gy-L	0.695	M-Or-Pe	0.729	M-Bl-Pe	0.473	M-Bd-Pe	0.168
M-Bd-Px	0.693	M-Bk-Pe	0.723	M-Gn-Pe	0.469	M-Bk-Pe	0.167
M-Br-Px	0.687	M-Bd-Pe	0.718	M-Bd2-Pr	0.467	T-Gy-L	0.161
M-Bk-Pe	0.682	M-Gy-Px	0.711	M-Or-Pr	0.467	M-Gy-Pe	0.159
M-Bd-Pe	0.679	M-Bd-Px	0.710	M-Re-Pr	0.465	M-Gy-Pr	0.157
M-Gy-Px	0.666	M-Br-Px	0.706	C-Re-0	0.464	M-Gs-Prc	0.156
M-Gy-Pr	0.621	M-Gy-Pr	0.668	M-Or-Pe	0.462	M-Gy-Px	0.151
M-Gs-Prc	0.609	M-Gs-Prc	0.656	T-Re-L	0.462	A-Gyc	0.143
M-Bl-Pe	0.605	M-Bl-Pe	0.613	C-Re-0c	0.462	M-Gs-Pr	0.143
M-Gd-Pe	0.583	M-Gd-Pe	0.586	M-Or-Px	0.461	T-Br-L	0.142
C-Bk-L	0.579	M-Gs-Pe	0.581	C-Or-C	0.460	M-Gl-Pr	0.141
M-Gs-Pe	0.570	C-Bk-L	0.567	M-Rd-Px	0.460	M-Bd-Px	0.139
M-Gy-Pe	0.543	M-Gy-Pe	0.554	C-Bk-C	0.459	M-Bk-Px	0.135
C-Bk-C	0.540	C-Bk-C	0.539	C-Gy-C	0.459	B-Gy	0.132
C-Gy-C	0.517	M-Gl-Pr	0.538	M-Rd-Pe	0.459	M-Br-Px	0.119
M-Gl-Pr	0.497	C-Gy-C	0.516	C-Bk-L	0.458	M-Gs-Pe	0.118

Different results were obtained by applying SFF algorithm (Tab. 2). The application of SFF has demonstrated that the following roof coverings have the strongest correlation with the asbestos-cement flat sheets (A-Gy): green engobed ceramic tile (C-Gn-C), purple metal sheets with polyurethane-polyamide coating (M-Bd2-Pr) and dark green metal sheets with poliester protective coating (M-Gn-Pe), while the least correlated roofing include: grey roofing felt (B-Gy), brown metal with polyurethane coating (M-Br-Px), and dark grey metal sheets coated with polyester (M-Gs-Pe). Spectral curve of asbestos-cement corrugated sheets has (A-Gyc) the highest correlation with those of grey cement tile (T-Gy), grey roofing felt (B-Gy), and light grey metal sheets with polyurethane-polyamide protective coating (M-Gl-Pr). The weakest correlation between asbestos-cement corrugated sheets (A-Gyc) and other roofing materials was recorded for grey engobed ceramic tile (C-Gy-C), ochre metal sheets coated with polyurethane-polyamide (M-Re-Pr), and black lacquered ceramic tile (C-Bk-L).

### 3.3. Differences in spectral reflection

#### Flat Asbestos-Cement Sheets

Difference in spectral reflectance greater than 0.1 between asbestos-cement flat sheets and the majority of other roofing is denoted within the whole tested range of the electromagnetic spectrum (500–2500 nm) (Fig. 8).

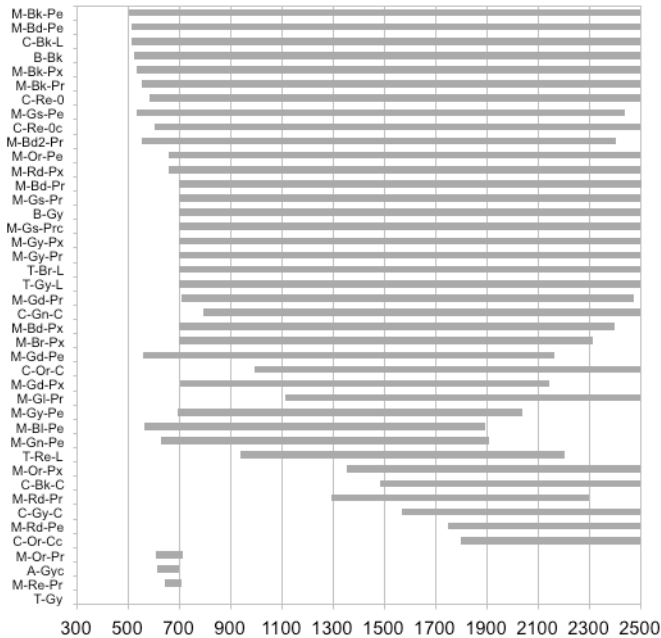
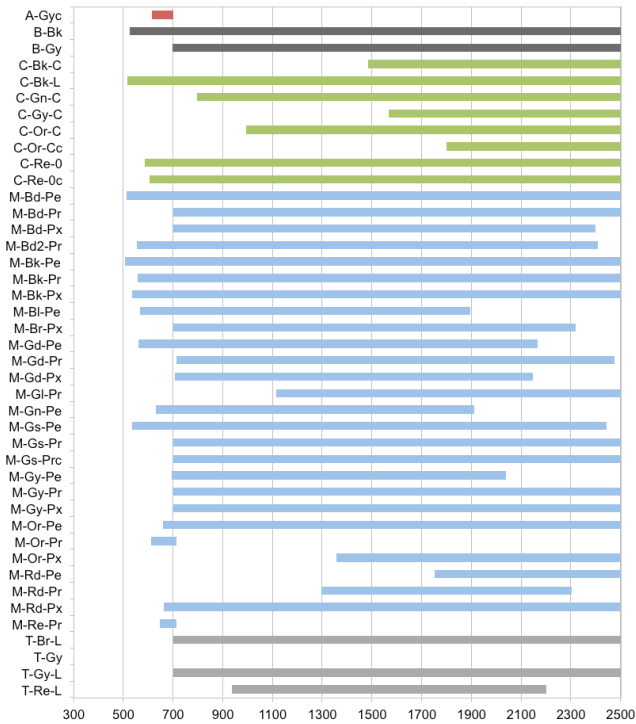


Fig. 8. Spectral reflectance difference value greater than 0.1 between asbestos-cement flat sheets and the other roof coverings arranged from largest to smallest interval reflectance values

The group consisted of engobed ceramic tiles, lacquered, copper ceramic tiles, and protected with polyurethane and polyamide coating discriminates from other roofing within the range between 1300–2500 nm. The exception in this group is graphite ceramic tile whose colour differs from others. Asbestos-cement corrugated sheets, grey concrete tile sheets, and copper metal sheet with the protective coating of polyurethane and polyamide differentiates only within the range of 600–700 nm.

Difference in spectral reflectance value between asbestos-cement flat sheets and other roofing materials greater than 0.1 (Fig. 9): asbestos-cement, roofing felt (black), clay (green), metal (blue), and concrete tile (grey), are very diverse. Protective coating made with cement and bitumen is characterized by a difference greater than 0.1 nearly in the entire wavelength range, with the exception of the concrete tile, wherein the difference in reflection throughout the range is less than 0.1. Large variations were observed for the colour of the roofing.



**Fig. 9.** Spectral reflectance difference values greater than 0.1 between asbestos-cement flat sheets, and other roof coverings arranged by composite material: red – asbestos, black – roofing felt, green – clay, blue – metal, grey – concrete tile

Maroon, copper, and ochre coatings are characterized by the greatest diversity in reflection, i.e. diverge by more than 0.1 Euclidean distance, in contrast to dark

coloured coating, i.e. dark brown, purple, black, dark grey, and grey, which were differentiating nearly in the entire spectrum range with a minimum value of 0.1 (Fig. 10). The exception is asbestos-cement corrugated sheets, tile, graphite, and black engobed ceramic tile.

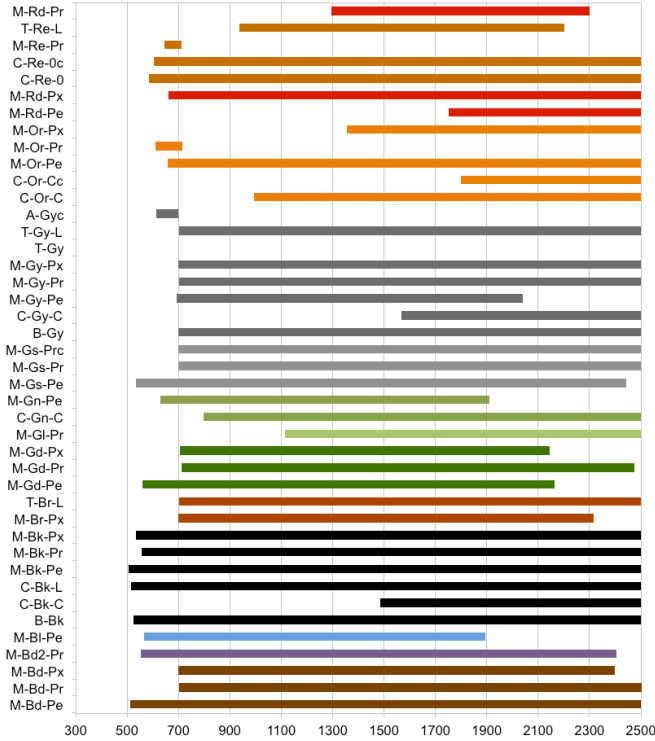


Fig. 10. Spectral reflectance value greater than 0.1 arranged by colour of roof covering

### Corrugated Asbestos-Cement Sheets

The difference in spectral reflectance between asbestos-cement corrugated sheets greater than 0.1 was denoted within a narrow range of electromagnetic spectrum (400–650 nm, 1800–1950 nm and 2400–2500 nm) (Fig. 11). As in the case of asbestos-cement flat sheets, concrete tile sheets differentiate from corrugated ACR within the narrow spectral range between 615 nm and 700 nm.

Roofing felt and concrete tile have a difference in spectral reflectance greater than 0.1 for almost the entire wavelength range, with the exception of natural concrete tile and copper concrete tile. Concrete tile, unlike asbestos-cement flat sheets, wherein the entire wavelength difference was less than 0.1 in reflectance, differentiates from asbestos-cement corrugated sheets in the spectral range from 650 nm to 1850 nm (Fig. 12).

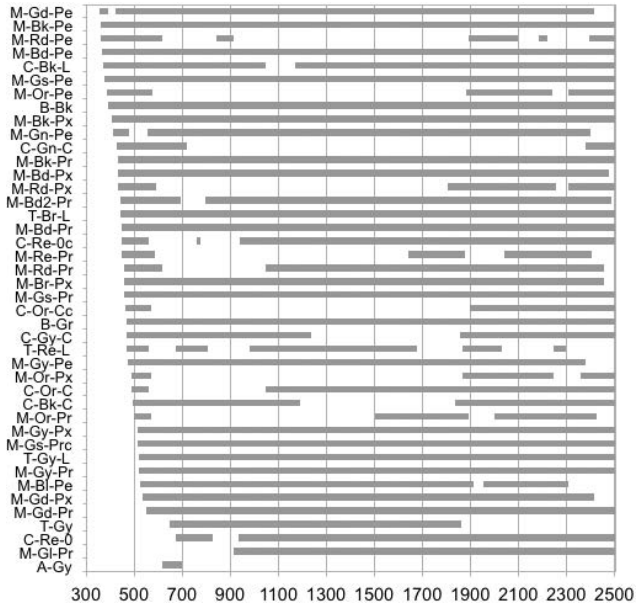


Fig. 11. Spectral reflectance greater than 0.1 between asbestos-cement corrugated sheets, and other roof coverings arranged from largest to smallest interval reflectance values

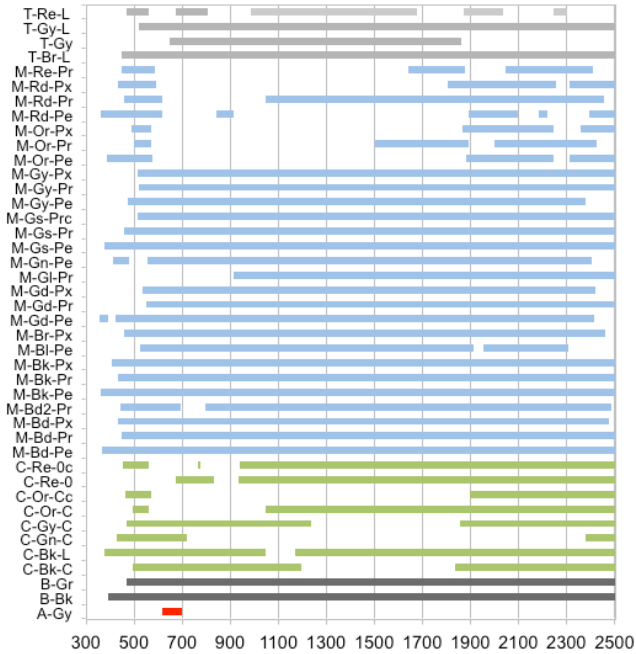


Fig. 12. Spectral reflectance value greater than 0.1 between asbestos-cement corrugated sheets, and other roof coverings arranged by composite materials (red – asbestos, black – roofing felt, green – clay, blue – metal, grey – concrete tile)

Metal sheets, except for coloured roofing (ochre, copper, maroon), differentiate in the tested spectrum. Spectral characteristic of red, maroon, and orange roofing are characterized by a great diversity of reflectance with the difference greater than 0.1. Two wavebands: 350–600 nm and 1900–2500 nm were distinguished. Other colour roofing differentiates from asbestos-cement corrugated sheets in the analysed spectrum (Fig. 13).

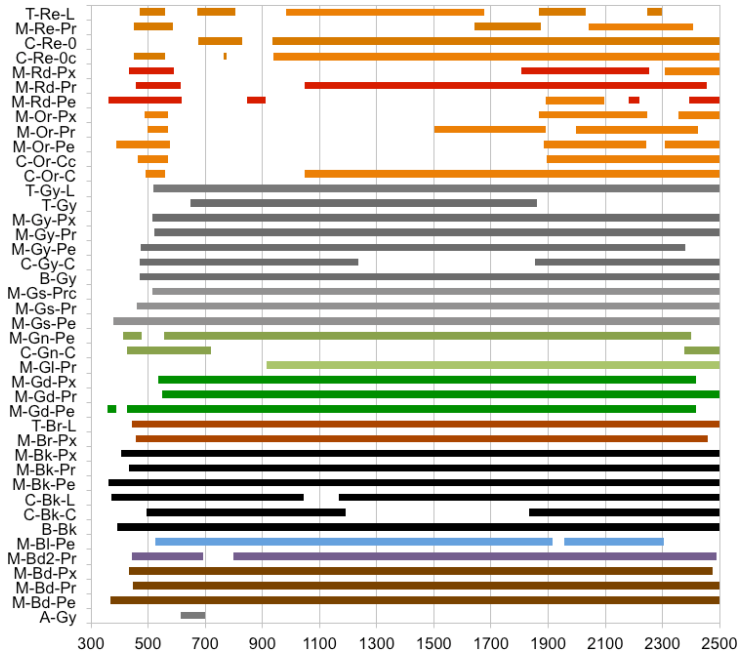
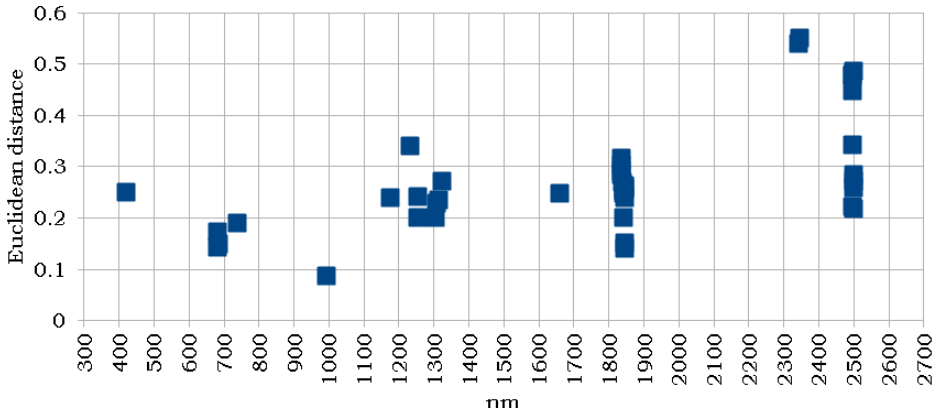


Fig. 13. Spectral reflectance value greater than 0.1 between asbestos-cement corrugated sheets, and other roof coverings arranged by composite materials (red – asbestos, black – roofing felt, green – clay, blue – metal, grey – concrete tile)

### 3.4. Wavelengths of the Maximum Spectral Reflectance Difference

The maximum difference in spectral reflectance of asbestos-cement flat sheet is 0.55 for dark brown polyester coating at the wavelength of 2344 nm, and maximum differences are grouped in the ranges of 680–740 nm (4 coverings), 1170–1320 nm (8 coverings), 1830–1850 nm (15 coverings), and 2340–2500 nm (12 coverings) (Fig. 14).

The maximum difference in spectral reflectance of asbestos-cement corrugated sheet is 0.51 for natural ceramic tile at the wavelength of 2497 nm, and maximum differences are grouped in ranges of 550–680 nm (4 coverings), 1230–1325 nm (5 coverings), 1670–1800 nm (23 coverings) and 2495–2500 nm (10 coverings) (Fig. 15).



**Fig. 14.** Maximum spectral reflectance difference between asbestos-cement flat sheets, and other roof covering

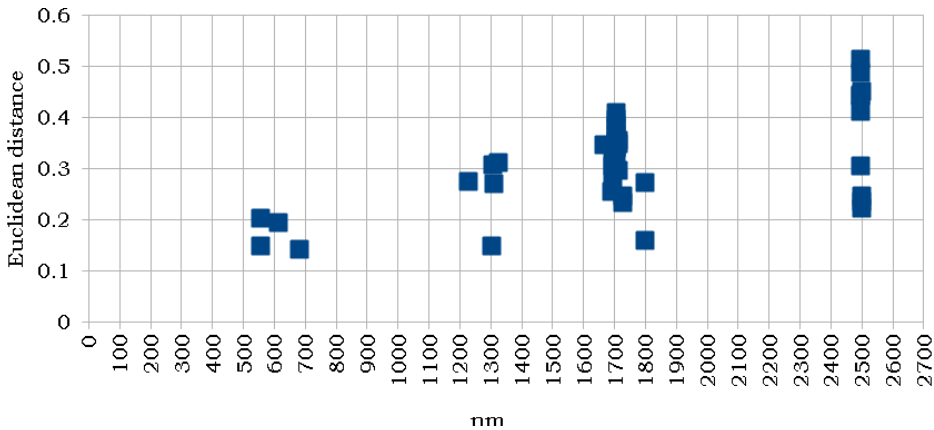


**Fig. 15.** Maximum spectral reflectance difference between asbestos-cement corrugated sheets and other roof coverings

The lowest value of the Euclidean distance indicates that concrete tile, asbestos-cement flat sheets, asbestos-cement corrugated sheets, ochre metal sheets, and copper metal sheets are the most similar types of roof covering. Major differences were denoted in spectral curves of roof coverings made of ceramic materials, without any protective coating.

#### 4. Discussion and Conclusions

Since roof coverings are made of different composite materials, shapes of spectral curves are very diverse. Groups of similar shape, and course of curves are perceivable. Significantly distinguishable spectral curves were denoted for metal sheet,

ceramic ochre, green, blue, and maroon tile. In order to discriminate asbestos from all other roofing materials, the whole spectral range should be examined.

Herold et al. [13] have classified buildings roofs among other urban areas taking into consideration the composite material, and colour of roofing, except of asbestos-cement sheets. It was determined that accuracy differences in roof type mapping were large, however, producer's and user's accuracy were increasing along with higher spectral resolution.

Asbestos roofing was discriminated by Fiumi et al. [8, 9] in Magliana Region (Italy) with the accuracy of 94.3%, where also composite materials typical for the region of interest were examined. Heiden et al. [11] in the east of Munich city centre (Germany) have proved that roofing materials can be discriminated due to their spectral features, however, asbestos-cement roofing was not distinguished as a separate class. Colours of coatings were also attributed in the survey as a part of image spectral library. Past surveys concerned urban land cover classification, in particular buildings roofing. Part of them involved discrimination of ACR or deterioration status of asbestos containing products. Current research indicates that discrimination of asbestos-cement roofing in Poland might be executed with the use of remote sensing data on hyperspectral imagery based on 3 different features: composite material, colour of material, and type of protective coating. Detailed study regarding the type of protective coating should be carried out, since it affects the shape of the spectral curve.

Band selection was done with the use of the correlation analysis; SAM and SFF algorithm application was enhanced by PCA. The following wavelengths were selected for asbestos discrimination in Poland: 410, 550, 670, 740, 870, 990, 1310, 1700, 1840, 2130, 2200, 2270 nm whereas local peaks, and the maximum difference in reflectance between asbestos and other roofing were examined. Water absorption within the range 1750–1950 nm prevents registration of this spectrum by satellite sensors, and it is a significant range in which about 16 roof coverings tested has maximum difference in reflectance. Further research will be undertaken to determine as to whether spectral differences can be used only for the low-level data (multispectral, hyperspectral, UAVs).

ACR may be distinguished from bituminous coverings, and dark-colour roof coverings, with a balanced low-reflection within the range of the spectrum. It appears to be harder to distinguish ACR from most of the coloured roof coverings (in the wavelength of 2500 nm ochre and copper roof tiles have a similar reflectance as asbestos-cement sheets), and natural concrete tile (cement unstained, unvarnished). It might be concluded that asbestos-cement corrugated sheets discriminates better than asbestos-cement flat sheets.

Spectral curves developed during the undertaken research are representative for new roof coverings. Under the influence of atmospheric conditions over time roofing materials are subject to change (modification of colours, cracks, overgrown with algae, mosses, lichens). Hence, these curves will not always be consistent with those prepared under laboratory conditions. In practice, the discrimination and



classification of ACR with the use of remote sensing data will depend on the spatial resolution, spectral, and radiometric resolution, and the number of training fields taking into consideration an issue of roofing angles (BRDF modelling). Discrimination of ACR from other roofing materials under the laboratory measurement, and development of spectral curves appears to be feasible, as confirmed by the analysis of spectral reflectance difference greater than 0.1, and application of SAM and SFF algorithms. After the analysis of spectral reflectance curves of individual roofing it may be stated that there is no apparent leading feature, such as: composite material, colour, or type of protective coating. Different spectral characteristics allows for ACR discrimination, however, further investigation should be carried out.

An estimation of the amount of asbestos-cement roofing is an important issue to attribute to the process of abatement and monitoring [8, 9, 17] due to the European Union legal regulations. Research has shown that it is possible to discriminate roof coverings with the use of hyperspectral data.

## References

- [1] *Act of 19 June 1997 on the prohibition of the use of asbestos-containing products*. Journal of Laws 1997, no. 101, item 628 as amended [*Ustawa z dnia 19 czerwca 1997 r. o zakazie stosowania wyrobów zawierających azbest*. Dz.U. 1997, nr 101, poz. 628].
- [2] Bassani C., Cavalli R.M., Cavalcante F., Cuomo V., Palombo A., Pascucci S., Pignatti S.: *Deterioration status of asbestos-cement roofing sheets assessed by analysing hyperspectral data*. Remote Sensing of Environment, no. 109, 2007, pp. 361–378.
- [3] Ben-Dor E., Levin N., Saaroni H.: *A spectral based recognition of the urban environment using the visible and near-infrared spectral region (0.4–1.1  $\mu\text{m}$ )*. A case study over Tel-Aviv, Israel. International Journal of Remote Sensing, vol. 22, no. 11, 2001, pp. 2193–2218.
- [4] Carvalho O.A. de, Meneses P.R.: *Spectral correlation mapper (SCM): an improvement on the spectral angle mapper (SAM)*. [in:] *Summaries of the 9th JPL Airborne Earth Science Workshop*, JPL Publication no. 9, Jet Propulsion Laboratory, National Aeronautics and Space Administration, 2000.
- [5] Collegium Ramazzini: *Asbestos is still with us: repeat call for a universal ban*. Odontology, no. 98, 2010, pp. 97–101.
- [6] *Commission Directive 1999/77/EC of 26 July 1999 adapting to technical progress for the sixth time Annex I to Council Directive 76/769/EEC on the approximation of the laws, regulations and administrative provisions of the Member States relating to restrictions on the marketing and use of certain dangerous substances and preparations (asbestos)*. [on-line:] <http://eur-lex.europa.eu/Notice.do?val=330332:cs&lang=pl&list=330332:cs,329492:cs,330564:cs,&pos=1&page=1&nbl=3&pgs=10&hwords=&checktexte=checkbox&visu=#texte> [access: 10.12.2015].

- [7] FieldSpec® Pro User's Guide, ASD Part #600000 Rev. C, 2002, Analytical Spectral Devices [on-line:] <http://support.asdi.com> [access: 10.12.2015].
- [8] Fiumi L., Congedo L., Meoni C.: *Developing expeditious methodology for mapping asbestos-cement roof coverings over the territory of Lazio Region*. Applied Geomatics, no. 6, 2014, pp. 37–48.
- [9] Fiumi L., Tocci S., Meoni C.: *Remote sensing and GIS for land use planning: an application for mapping asbestos cement roofing in Tiburtina, Rome, Italy*. International Journal of Remote Sensing & Geoscience (IJRSG), vol. 3, no. 3, 2014, pp. 1–9.
- [10] Frassy F., Candiani G., Rusmini M., Maianti P., Marchesi A., Nodari F.R., Dalla Via G., Albonico C., Gianinetto M.: *Mapping Asbestos-Cement Roofing with Hyperspectral Remote Sensing over a Large Mountain Region of the Italian Western Alps*. Sensors, vol. 14, 2014, pp. 15900–15913.
- [11] Heiden U., Heldens W., Roessner S., Segl K., Esch T., Mueller A.: *Urban structure type characterization using hyperspectral remote sensing height information*. Landscape and Urban Planning, no. 105, 2012, pp. 361–375.
- [12] Heiden U., Segl K., Roessner S., Kaufmann H.: *Determination of robust spectral features for identification of urban surface materials in hyperspectral remote sensing data*. Remote Sensing of Environment, no. 111, 2007, pp. 537–552.
- [13] Herold M., Gardner M.E., Roberts D.A.: *Spectral Resolution Requirements for Mapping Urban Areas*. IEEE Transactions on Geoscience and Remote Sensing, no. 41, 2003, pp. 1907–1919.
- [14] Herold M., Roberts D., Gardner M., Dennison P.: *Spectrometry for urban area remote sensing – Development and analysis of a spectral library from 350 to 2400 nm*. Remote Sensing of Environment, no. 91, 2004, pp. 304–319.
- [15] IBAS (International Ban Asbestos Secretariat), 2014. [on-line:] [http://www.ibasecretariat.org/lka\\_alpha\\_asb\\_ban\\_280704.php](http://www.ibasecretariat.org/lka_alpha_asb_ban_280704.php) [access: 10.12.2015].
- [16] ILO (International Labour Organisation), and WHO (World Health Organisation): *Outline for the Development of National Programmes for Elimination of Asbestos-Related Diseases*. 2007. [on-line:] [http://www.who.int/occupational\\_health/publications/Out\\_NPEAD\\_ENG.pdf](http://www.who.int/occupational_health/publications/Out_NPEAD_ENG.pdf) [access: 10.12.2015].
- [17] Krówczyńska M., Wilk E.: *Aerial imagery and geographic information systems used in the asbestos removal process in Poland*. [in:] Lasaponara R., Masini N., Biscione M. (ed.), *33th EARSeL Symposium Towards Horizon 2020: Earth Observation and Social Perspectives*, Matera, Italy FARSEL and CNR, 2013, pp. 823–828.
- [18] Krówczyńska M., Wilk E., Zagajewski B.: *The Electronic Spatial Information System – tools for the monitoring of asbestos in Poland*. Miscellanea Geographica – Regional Studies On Development, vol. 18, no. 2, 2014, pp. 59–64.
- [19] Kycko M., Zagajewski B., Podbielska K., Binkowska A.: *Wpływ geometrii źródła promieniowania-roślina-detektor na wartość teledetekcyjnych wskaźników roślinności*. Teledetekcja Środowiska, t. 49, 2013, pp. 15–26.

- [20] LaDou J., Castleman B., Frank A., Gochfeld M., Greenberg M., Huff J., Joshi T.K., Landrigan P.J. et al.: *The Case for a Global Ban on Asbestos*. Environmental Health Perspectives, vol. 118, no. 7, 2010, pp. 897–901.
- [21] Marino C., Panigada C., Busetto L.: *Airborne hyperspectral remote sensing applications in urban areas: asbestos concrete sheeting identification and mapping*. IEEE/ISPRS, 2001, pp. 212–216.
- [22] Meer F. van der: *Analysis of spectral absorption features in hyperspectral imagery*. International Journal of Applied Earth Observation and Geoinformation, vol. 5, no. 1, 2004, pp. 55–68.
- [23] *Ordinance of the Minister of Economy of 13 December 2010 on requirements for the use of products containing asbestos and the use and cleaning of plant or equipment, which have been or are being used asbestos-containing products*. Journal of Laws 2011, vol. 8, item 31 [Rozporządzenie Ministra Gospodarki z dnia 13 grudnia 2010 r. w sprawie wymagań w zakresie wykorzystywania wyrobów zawierających azbest oraz wykorzystywania i oczyszczania instalacji lub urządzeń, w których były lub są wykorzystywane wyroby zawierające azbest. Dz.U. 2011, nr 8, poz. 31].
- [24] Polish Industry Standard [Norma Branżowa] BN-67/6754-02. *Azbest chryzotylowy do produkcji wyrobów azbestowo-cementowych*.
- [25] *Programme for Asbestos Abatement in Poland 2009–2032*. Resolution No. 39/2010 of the Council of Ministers of 15 March 2010 [Program oczyszczania kraju z azbestu na lata 2009–2032. Załącznik do uchwały nr 39/2010 Rady Ministrów z dnia 15 marca 2010 r.]. [on-line:] [http://www.mg.gov.pl/files/upload/8369/PROGRAM\\_ENG.pdf](http://www.mg.gov.pl/files/upload/8369/PROGRAM_ENG.pdf) [access: 14.12.2015].
- [26] Segl K., Roessner S., Heiden U., Kaufmann H.: *Fusion of spectral and shape feature for identification of Urban surface cover types using reflective and thermal hyperspectral data*. Photogrammetry and Remote Sensing, no. 58, 2003, pp. 99–112.
- [27] Szabó S., Burai P., Kovács Z., Szabó G., Kerényi A., Fazekas A., Paládi M., Buday T., Szabó G.: *Testing of Algorithms for the Identification of Asbestos Roofing Based on Hyperspectral Data*. Environmental Engineering and Management Journal, 2014, vol. 143, no. 11, pp. 2875–2880.
- [28] Virta R.L.: *Asbestos: Geology, Mineralogy, Mining, and Uses*. U.S. Department of the Interior, U.S. Geological Survey, Open-File Report 02-149. [on-line:] <http://minerals.usgs.gov/minerals/pubs/commodity/asbestos/> [access: 10.12.2015].
- [29] Ward J.H., Jr., *Hierarchical Grouping to Optimize an Objective Function*. Journal of the American Statistical Association, 1963, vol. 58, pp. 236–244.
- [30] Wilk E., Krówczyńska M., Zagajewski B.: *Asbestos manufacturing plants in Poland*. Miscellanea Geographica – Regional Studies On Development, vol. 18, no. 2, 2014, pp. 53–58.